Anderson transition in ultracold atoms: Signatures and experimental feasibility

Antonio M. García-García
Physics Department, Princeton University, Princeton, New Jersey 08544, USA and The Abdus Salam International Centre for Theoretical Physics, P.O. Box 586, 34100 Trieste, Italy

Jiao Wang
Department of Physics, National University of Singapore, 117542 Singapore and Beijing-Hong Kong-Singapore Joint Center for Nonlinear and Complex Systems (Singapore), National University of Singapore, 117542 Singapore

(Received 28 August 2006; published 29 December 2006)

Kicked rotators with certain nonanalytic potentials avoid dynamical localization and undergo a metal-insulator transition. We show that typical properties of this transition are still present as the nonanalyticity is progressively smoothed out provided that the smoothing is less than a certain limiting value. We have identified a smoothing-dependent time scale such that full dynamical localization is absent and the quantum momentum distribution develops power-law tails with anomalous decay exponents as in the case of a conductor at the metal-insulator transition. We discuss under what conditions these findings may be verified experimentally by using ultracold atom techniques. It is found that ultracold atoms can indeed be utilized for the experimental investigation of the metal-insulator transition.

DOI: 10.1103/PhysRevA.74.063629 PACS number(s): 03.75.Lm, 72.15.Rn, 05.45.Pq, 05.45.−a

I. INTRODUCTION

The study of a quantum particle in a random potential [1] is one of the cornerstones of modern condensed matter physics. In its simplest form—namely, a free spin-less particle in a short-range disordered potential with no interactions at zero temperature—the combination of the one-parameter scaling theory [2], the supersymmetry method [3], and numerical simulations [4] has led to the following picture: In two and lower dimensions destructive interference caused by backscattering produces exponential localization of the eigenstates in real space for any amount of disorder. As a consequence, quantum transport is suppressed, the spectrum is uncorrelated (Poisson), and the system becomes an insulator. In more than two dimensions there exists a metal insulator transition [usually referred to as the Anderson transition (AT)] for a critical amount of disorder. By critical disorder we mean a disorder such that, if increased, all the eigenstates become exponentially localized. For a disorder strength below the critical one, the system has a mobility edge at a certain energy which separates localized from delocalized states. Its position moves away from the band center as the disorder is decreased. Delocalized eigenstates, typical of a metal, are extended through the sample, and level statistics agrees with the random matrix prediction for the appropriate symmetry. In three and higher dimensions the AT takes place in a region of strong disorder only accessible to numerical [4,5] simulations. Typical features of the AT include the following.

(i) Scale invariance [6] of the spectrum; namely, any spectral correlator utilized to describe the spectral properties of the disordered Hamiltonian does not depend on the system size. The spectral correlations at the AT, usually referred to as critical statistics [6,7], are intermediate between that of a metal and that of an insulator.

(ii) Anomalous scaling of the eigenfunction moments, $\mathcal{P}_q=\int d^d r|\psi(\mathbf{r})|^{2q}\propto L^{-D_q(q-1)}$, with respect to the sample size L, where D_q is a set of exponents describing the AT. Eigenfunctions with such a nontrivial (multi)scaling are usually dubbed multifractals [5] (for a review see [8]).

(iii) Quantum diffusion is anomalous [9] at the AT. In the metallic limit, up to small weak localization corrections, the density of probability is Gaussian like and the dynamics is well described by a Brownian motion. However, as disorder increases, localization effects become important and quantum diffusion slows down. The density of probability develops power-law tails with a decay exponent depending on the spectrum of multifractal dimensions [9].

Unfortunately the experimental verification of the AT is a challenging task. In the context of electronic systems is extremely hard to disentangle effects caused by short decoherence times, electron-electron interactions, and phonon-electron interactions from destructive quantum interference, supposed to be the main ingredient driving the AT.

In recent years ultracold atoms in optical lattices [10] has been utilized to model certain solid-state physics systems. Generically, in these experiments a very dilute almost free gas of atoms (Cs and Rb) is cooled up to temperatures of the order of tens of microkelvins and then interacts with an optical lattice. In its simplest form, the optical lattice consists of two laser beams prepared in such a way that the resulting interference pattern is a stationary plane wave in space. The laser frequency is tuned close to a resonance of the atomic system in order to enhance the atom-laser coupling but not too close to avoid spontaneous emission. In this limit the laser-atom system can be considered as a point particle in a sine potential—namely, the quantum pendulum. Additionally, if the laser is turned on only in a series of short periodic pulses, the resulting system is very well approximated by the so-called quantum kicked rotor (see [11] for a review) extensively studied in the context of quantum chaos,

$$\mathcal{H}=p^2/2+k\cos(q)\sum_n \delta(t-Tn). \tag{1}$$

The classical motion of this system is diffusive in momentum space. For short time scales, quantum and classical mo-

tions agree. However, quantum diffusion is eventually suppressed due to interference effects and eigenstates are exponentially localized in momentum space. This counterintuitive feature, usually referred to as dynamical localization [12], was fully understood [13] after mapping the kicked rotator problem onto an short-range one-dimensional (1D) disordered system where localization is well established. The first direct experimental realization of the kicked rotor was reported in Ref. [10]. As was expected, the output of the experiment (the distribution of the atom momentum and the energy diffusion as a function of time) fully agrees with the theoretical prediction of dynamical localization [13]. Finally we remark that, after the pioneering work of Ref. [10], many other aspects of the physics of a quantum kicked rotor such as the effect of noise and dissipation have also been investigated [15] by using similar experimental settings.

The above results do not depend on the exact details of the potential but only on its ability to produce classical chaotic motion. The situation is different if the potential is not smooth. Recently [16], it has been reported that a kicked rotor could avoid full dynamical localization if the smooth sinusoidal optical potential is replaced with a generic potential with a logarithmic or steplike singularity. It was found that, for these potentials, the kicked particle has striking similarities with a free particle in a disordered potential at the AT. Thus level statistics are given by critical statistics, eigenfunctions are multifractal, and quantum diffusion becomes anomalous.

A natural question to ask is whether this nonanalytical kicked rotor can be realized in experiments. If so, this would be an ideal setting to test the physics of the AT. We notice that this is far from evident. Other similar proposals [14] turned out hard to implement in the laboratory.

Obviously, in experiments the singularity can only be approximated. For instance, an optical lattice potential with an approximate steplike singularity can be produced [18] either by a holographic mask [19] with precision σ or by adding a limited number of Fourier components. In both cases the potential is smooth on sufficiently small scales $\sim\sigma$. That means that for momenta $p_d \gg \hbar/\sigma$ and times t_d sufficiently long, the microscopic smoothness of the potential is at work and standard dynamical localization should be observed. On the other hand, for momenta p_c and times t_c sufficiently short, classical and quantum results should coincide. In between these two scales typical properties of the AT are observed. The aim of this paper is twofold: on the one hand, we seek to determine in what window of σ the AT is observed. On the other hand, we examine whether this range is already experimentally accessible by using ultracold atoms in optical lattices.

The organization of the paper is as follows: In the next section we introduce a kicked rotor with two different smoothed out versions of a step potential. Then we evaluate the rate of energy diffusion and the full momentum distribution. Finally we establish the minimum smoothing required to observe the AT and whether an experimental verification is realistic with the current, state-of-the-art, ultracold atom techniques.

II. MODEL AND OBSERVABLES

We investigate a kicked rotor in 1+1D with a smoothed steplike potential,

$$\mathcal{H} = \frac{p^2}{2} + V_{1,2}(q)\sum_n \delta(t-nT), \tag{2}$$

with $q \in [-\pi, \pi)$. We consider the following two potentials:

$$V_1(q) = \mathrm{Si}\left(\left(\frac{\pi}{2}+q\right)\Big/\sigma\right) + \mathrm{Si}\left(\left(\frac{\pi}{2}-q\right)\Big/\sigma\right), \tag{3}$$

where $Si(q)=\int_0^q \frac{\sin(t)}{t}dt$ is the sine integral function and

$$V_2(q) = \sum_{m=0}^{M} f(m)\cos(mq), \tag{4}$$

where $f(m)$ is the discrete Fourier transform of the bare steplike potential $V(q)=\pi$ for $|q|<\pi/2$ and zero otherwise. In both cases for $\sigma\to 0$ ($\sigma\equiv 1/M$ in the latter case) we recover the bare steplike potential investigated in [16]. There are infinitely many ways to smooth a singularity. We have chosen the above two due to similarities with the experimental situation. Thus $V_1(q)$ represents an optical lattice with square-wave intensity profile as produced by an array of fine slits or a holographic mask [19]. The other potential $V_2(q)$ produces an approximated steplike shape by adding a limited number of Fourier components. We remark that results for $V_1(q)$ and $V_2(q)$ are hardly distinguishable; both are smooth and oscillatory on scales of the order of σ. Numerically it is a little easier to simulate $V_1(q)$, so we will stick to it for our calculations.

We analyze both the classical and quantum motions of the above Hamiltonian. The classical evolution over a period T is dictated by the map $p_{n+1}=p_n-\frac{\partial V(q_n)}{\partial q_n}$, $q_{n+1}=q_n+Tp_{n+1}$ (mod 2π). By smoothing the step potential the classical force has a well-defined classical limit for any finite σ.

The quantum dynamics is governed by the quantum evolution operator $\mathcal{U}$ over a period T. Thus, after a period T, an initial state ψ_0 evolves to $\psi(T)=\mathcal{U}\psi_0=e^{-i\hat{p}^2T/2\hbar}e^{-iV(\hat{q})/\hbar}\psi_0$ where $\hat{p}$ and $\hat{q}$ stand for the usual momentum and position operators. Our aim is to evolve a given initial state to a certain time nT. This is equivalent to solving the eigenvalue problem $\mathcal{U}\Psi_n=e^{-i\kappa_n/\hbar}\Psi_n$ where Ψ_n is an eigenstate of $\mathcal{U}$ with quasieigenvalue κ_n. In order to proceed we can express the evolution operator $\langle m|\mathcal{U}|n\rangle=U_{nm}$ in the basis of momentum eigenstates $\{|n\rangle=\frac{e^{in\theta}}{\sqrt{2\pi}}\}$ with $n=0,\ldots,N\to\infty$,

$$U_{mn} = \frac{e^{-i(T\hbar/4)(m^2+n^2)}}{2\pi}\int_{-\pi}^{\pi} dq e^{iq(m-n)-iV(q)/\hbar}. \tag{5}$$

We remark that in this representation, referred to as the "cylinder representation," the resulting matrix U_{nm} is unitary exclusively in the $N\to\infty$ limit. This is certainly a disadvantage since besides typical finite-size effects one has also to face truncation effects; namely, the integral of the density of probability is not exactly unity and eigenvalues are not pure phases ($e^{-i\theta_n}$) as expected in a unitary matrix. Moreover, the

diagonalization of a generic nonunitary matrix is numerically much more demanding.

These difficulties can be circumvented by changing representations in each quantum iteration step, a technique extensively adopted in quantum kicked rotator studies. First, we express a given state ψ in position representation, so that it is straightforward to get $\psi' = e^{-iV(\hat{q})/\bar{h}}\psi$, the state just after the kick. Next, we express ψ' in the angular momentum representation by using the fast Fourier transformation (FFT) algorithm to facilitate the calculation of $e^{-i\hat{p}^2T/2\bar{h}}\psi'$. Since no matrix diagonalization is involved in this scheme, the computation is quite fast and the effective dimension of the state vectors is as large as 10^8. As a result the truncation effects mentioned above can be safely neglected. We recall that this method allows us to resolve the potential with a precision of 10^{-8}, four orders less than the minimum $\sigma(10^{-4})$ investigated. Such a degree of precision is a necessary requirement to determine the effect of a small σ in the quantum transport properties of the model studied.

Analytical results for the above model can in principle be obtained by mapping Eq. (2) onto a 1D Anderson model. This method was introduced in [13] for the case of a kicked rotor with a smooth potential. We do not repeat here the details of the calculation but just state how the 1D Anderson model is modified by the nonanalytical potential. It turns out that the classical nonanalyticity induces long-range disorder in the associated 1D Anderson model. If the kick strength is sufficiently large, the diagonal part of the Anderson model is pseudorandom and the off-diagonal one decays as $U_r \sim 1/r$ with r the distance from the diagonal. This Anderson model is similar to the one studied in [5] which is solved by using the supersymmetry method. In general, according to Ref. [5], a $1/r$ decay in 1D is the signature of an AT. For the potential $V_{1,2}$ above, it is straightforward to show that $U_r \sim 1/r$ for $r \ll 1/\sigma$ and $U_r \sim e^{-\sigma r}$ for $r > 1/\sigma$. Consequently we expect to observe AT-like behavior for small momentum and then eventually recover the results of the sinusoidal potential—namely, exponential localization in momentum space. For further details of the analytical approach we refer to [16].

We are mainly interested in observables related to transport properties as the density of probability and the rate of diffusion.

The density of probability of finding a particle with momentum p after a time t for a given initial state $|\psi(0)\rangle = |0\rangle$. $P_q(p,t) \equiv P_q(k,t) = |\langle k|\phi(t)\rangle|^2$ with $p = k\hbar$. In all calculations we set $\hbar = 1$. The classical $P(p,t)$ is obtained by evolving the classical equation of motion for 2×10^7 different initial conditions with zero momentum $p=0$ and uniformly distributed positions along the interval $(-\pi, \pi)$. We would like to emphasize our results do not depend on the initial conditions. For instance, we have obtained similar results if the initial conditions of Ref. [17] are utilized.

We also examine the second moment of the probability distribution—namely, the energy diffusion $\langle p^2(t)\rangle = \int_0^\infty dp p^2 P(p,t)$ as a function of time.

We recall our aim is to find out whether the transport properties are compatibles with those of a disordered conductor at the AT and how they are affected by the short-distance differentiability of the potential. For the sake of completeness let us briefly summarize the predictions for both a kicked particle in a smooth potential and a disordered conductor at the AT.

For a kicked rotator with a smooth potential, it is well established that initially (up to a certain time t_c) both classical and quantum probabilities are Gaussian like and the diffusion in momentum is normal—namely, a standard Brownian motion. For longer times the classical density of probability is still that of a normal diffusion process. However, $P_q(p,t)$ become exponentially localized and energy diffusion stops $\langle p^2(t)\rangle \sim$ const. These are typical signatures of dynamical localization.

At the AT, up to a certain t_c, agreement is also expected between the classical and quantum predictions. In the case of a disordered conductor the classical dynamics is obviously well described by a Brownian motion. However, for $t > t_c$, the diffusion becomes anomalous, the quantum density of probability develops power-law tails in space (localization in a disordered conductor occurs in real space), and time with exponents related to the multifractal dimensions of the eigenstates [9]. The rate of diffusion is in some cases still similar to the one corresponding to normal diffusion $\langle p^2(t)\rangle = D_{quan}t$, though the quantum diffusion constant D_{quan} is typically lower. This suggests that, at the AT, destructive interference is still at work but it is not sufficient to fully localize the particle. In our case we also expect agreement between classical and quantum results up to a certain time $t_c(\sigma)$. Additionally, since the potential is differentiable for distances smaller than the smoothing σ, we expect that there exists a $t_d(\sigma)$ such that for $t \gg t_d$ standard dynamical localization becomes dominant.

Typical features of the AT transition are thus observed in our model only if $t_c \ll t_d$. It is unclear for what range of σ, $t_d \gg t_c$ and whether these values of σ can be reached experimentally. We answer these questions in the next section.

III. RESULTS

For the sake of clearness we first enunciate our main conclusions.

(i) Typical features of an AT are observed for $\sigma \leqslant 0.05$ and $t_c \gg t \gg t_d$.

(ii) The quantum-classical breaking time t_c remains almost unchanged with σ. In the range of σ investigated $t_c \leqslant 10$. By contrast, the time scale signaling the beginning of full dynamical localization, due to the differentiability of the potential, increases as σ decreases, $t_d \approx 2/\sigma$.

(iii) The above range of parameters is accessible to experimental verification. By using holographic mask techniques one can reach up to $\sigma \sim 0.01$ [18]. On the other hand, coherence in ultracold atoms is maintained well beyond 1000 kicks. Consequently the AT can be investigated by using ultracold atoms in optical lattices.

We have computed (see details in previous section) the quantum and classical density of probability for the Hamiltonian (2) with potentials given by Eq. (3) and a variety of smoothings $\sigma \in [0.1, 10^{-4}]$.

Our first task is to determine t_c and t_d as a function of σ. These time scales can in principle be calculated by using

different observables. Qualitatively all observables should provide the same physical picture. However, the numerical value of t_c and t_d may depend on the observable considered. For the sake of simplicity we estimate these time scales by looking at the rate of energy diffusion $\langle p^2(t)\rangle$.

A. Energy diffusion

Classically as initial conditions we use $p_0=0$ and q_0 a random number from the interval $[-\pi,\pi]$. Obviously only initial conditions in the narrow region $[-\pi+\sigma,\pi-\sigma]$ get a sizable kick. Thus even after several kicks there is a high probability that the system stays in the region $p=0$. In order to show that our results are not sensitive to initial conditions and stable under perturbations we have added a weak noise $V(q)=k\sin(q)$ with $k=1$. We have not observed any dependence on k provided $k\ll 1/\sigma$. For $k\sim 1/\sigma$ the effect of the pseudosingularity is obscured by the noise strength.

In the classical case (see Fig. 1) $\langle p^2(t)\rangle$ increases linearly with time. The dependence of the diffusion coefficient on σ is well approximated by $D=0.5/\sigma$. This is consistent with the analytical prediction resulting from the random phase approximation [20]. In the quantum case (see Fig. 1) we distinguish three different regions. In a first stage ($t<t_c \leqslant 10$) the quantum-averaged energy agrees with its classical counterpart. The breaking time t_c depends quite weakly on σ. For longer times $t_c<t<t_d$, the diffusion is still similar to the classical case, $\langle p^2(t)\rangle \approx D_{quan}t$, with $D_{quan}\sim 0.2/\sigma$. However, though dependence on σ is the same, the numerical value of the diffusion coefficient is smaller than the classical one. This suggests that quantum interference effects slow down the classical diffusion. A similar feature has been found in a disordered conductor at the AT [9]. This stage lasts up to $t_d \approx 2/\sigma$. For longer times standard dynamical localization due to the differentiability of the potential takes over and diffusion stops.

We recall that $\langle p^2(t)\rangle\sim t$ is only a necessary condition for normal diffusion. In general, the information obtained from the knowledge of a few moments of the distribution is not sufficient to fully characterize the classical motion. For instance, the second moment may be $\langle p^2(t)\rangle\sim t$ but this by no means assures that the density of probability is Gaussian like [21]. We show below that this is precisely the case in our model.

B. Density of probability

We distinguish the following two regions in the classical density of probability (see Fig. 2): First, for short time scales (a few kicks) and $|p|<c(\sigma)\sqrt{2Dt}$ the diffusion is anomalous. $P(p,t)\sim p^{-\alpha}$ with $\alpha\sim 2$ and $c(\sigma)\approx 1$ slightly increases as σ decreases. For such a short time scale the classical system does not feel the differentiability of the potential. The observed wiggling for $p'>1$ is a direct consequence of the strong oscillations of the potential (3) in the region close to the edges of the smoothed step potential.

For longer times but $t<t_d$, we observe a gradual crossover from anomalous to normal diffusion. For small momentum the density is still non-Gaussian as the effect of the pseudonondifferentiability is still important. As time approaches t_d, the central (small momentum) non-Gaussian region becomes smaller and smaller. Meanwhile, the outskirts bend down and a Gaussian-like behavior typical of normal diffusion is observed. Finally, for $t>t_d$, $P(p,t)$ is well approximated by a Gaussian distribution. These regions have been observed for all σ of interest.

To evaluate $P(p,t)$, we count the number of systems whose momentum falls in $(p-\Delta p/2, p+\Delta p/2)$ at time t, then approximate $P(p,t)$ with the its ratio to the size of the ensemble. For the calculations in Fig. 2 we set $\Delta p=0.03\sqrt{2Dt}$ and the corresponding $\Delta p'=0.03$.

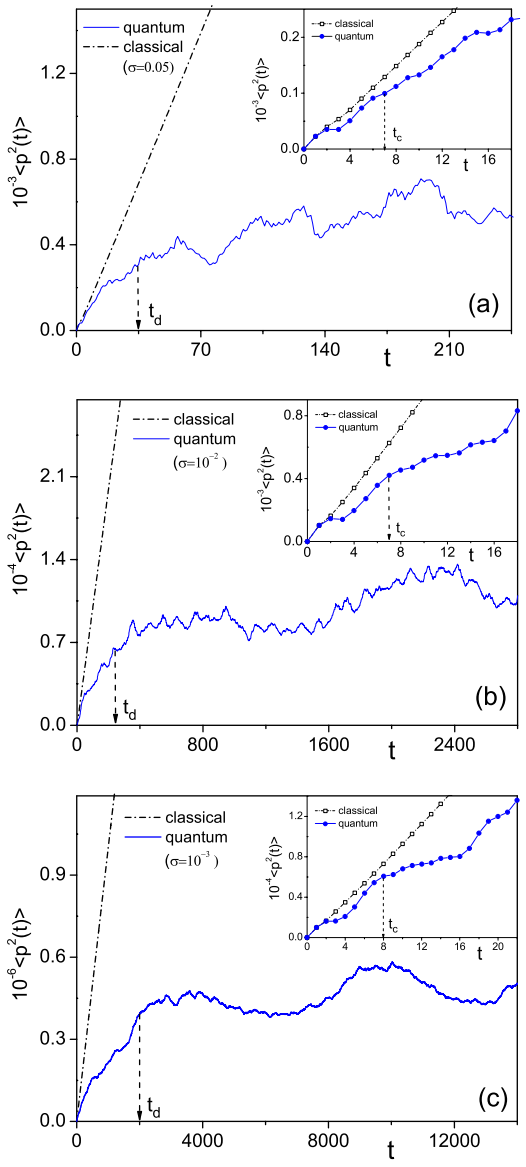

FIG. 1. (Color online) Comparison of quantum and classical energy diffusion versus time (number of kicks) for different smoothings: $\sigma=5\times10^{-2}$ (a), $\sigma=10^{-2}$ (b), and $\sigma=10^{-3}$ (c). The quantum initial condition $|\psi(0)\rangle=|0\rangle$ was chosen to mimic its classical counterpart. For $t<t_c$ quantum and classical diffusion rates are similar. For $t_d\approx 2/\sigma$ the quantum energy diffusion gets saturated due to destructive interference. In between these two scales the system behaves as a disordered conductor at the AT.

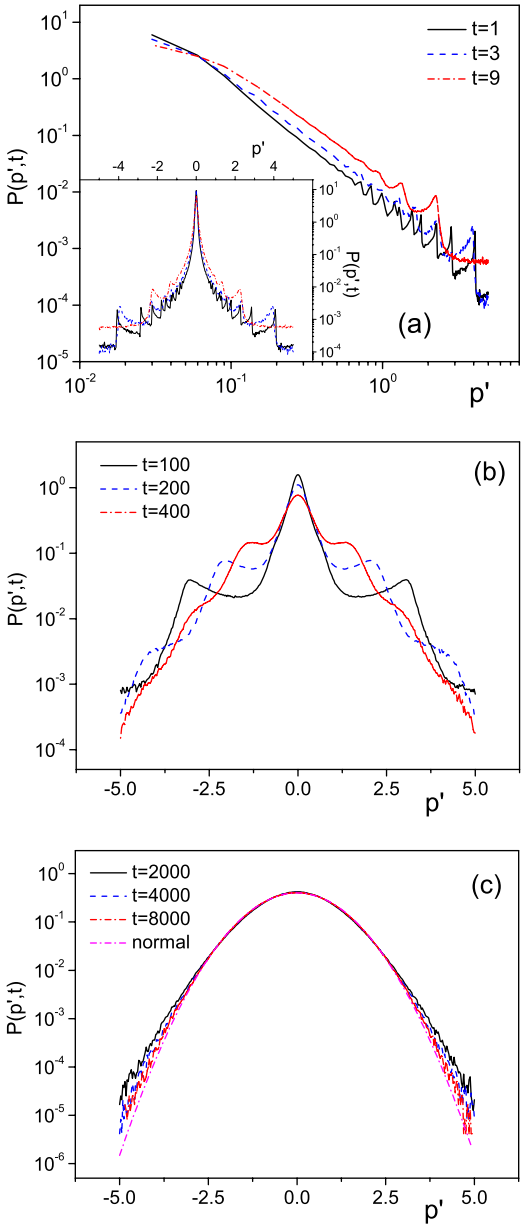

FIG. 2. (Color online) Classical density of probability distribution $P(p',t)$ for $\sigma=10^{-3}$ and $p'=p/\sqrt{2Dt}$. (a) Region of anomalous diffusion, $t<10$, (b) crossover from anomalous to normal diffusion $10<t<t_d\approx 2/\sigma$, and (c) normal diffusion $t>t_d$. The results were obtained after averaging over 2×10^7 initial conditions.

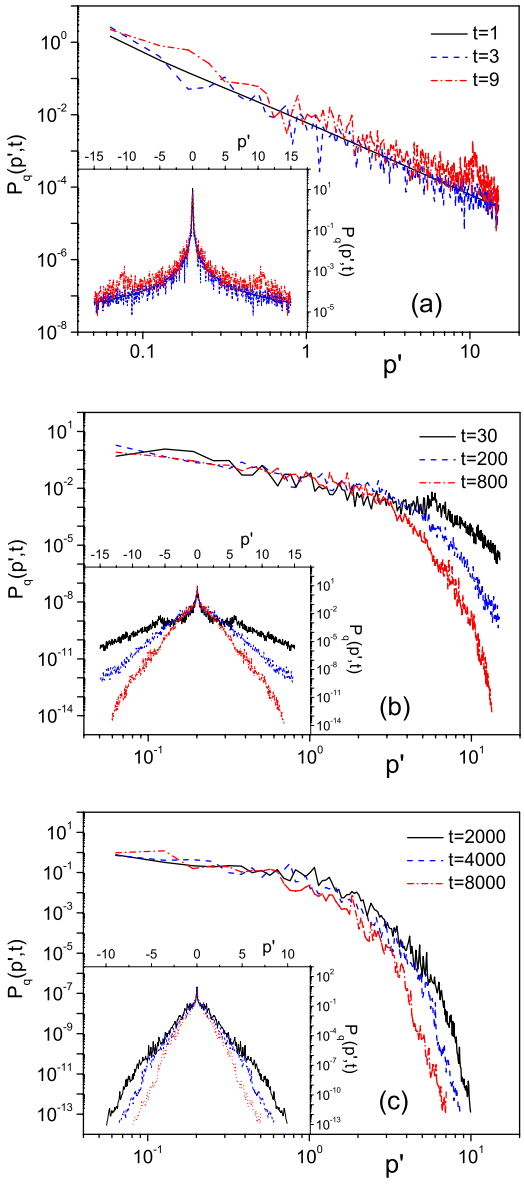

FIG. 3. (Color online) Quantum density of probability distribution $P_q(p',t)$, $p'=p/\sqrt{2Dt}$ and $\sigma=10^{-3}$ for three different regions: (a) $t<t_c\leqslant 10$, agreement between classical and quantum results, (b) $t_c<t<t_d$, typical properties of an AT are observed, and (c) $t>t_d$, standard dynamical localization for $|p|>\sqrt{2Dt_d}$. In the insets we present the same results in a linear-log scale. $P_q(p',t)\sim 1/p^2$ for $t<t_c$ and $|p|'<1$, and $P_q(p',t)\sim 1/p^\alpha$ with $\alpha=1.1\pm 0.2$ for $t>t_c$. As initial condition we used $|\psi(0)\rangle=|0\rangle$.

In the quantum case three regions are distinguished (see Fig. 3).

(i) $t<t_c$ and $|p|<c(\sigma)\sqrt{2Dt}$ with $D\approx 0.5/\sigma$ [$c(\sigma)$ increases slightly as σ decreases]. In agreement with the results on energy diffusion (see Fig. 1) both classical and quantum probabilities also agree in this region (see Fig. 4). The time scale t_c depends also weakly on σ. This is not surprising since our system has not a well-defined classical-quantum correspondence in the limit $\sigma\to 0$. The diffusion is also anomalous, $P_q(p,t)=P(p,t)\sim 1/p^2$. As in the classical case, $P_q(p,t)$ was calculated by summing up the probability falling in a bin of width Δp. We set $\Delta p=2\sqrt{t}$ (corresponding $\Delta p'=2/\sqrt{2D}\approx 0.063$) for Fig. 3; hence, it is in fact a coarse-grained result where part of the quantum fluctuations have been suppressed.

(ii) For $|p|<c(\sigma)\sqrt{2Dt}$ but $t_d>t>t_c$. The quantum probability $P_q(p,t)\sim 1/p^\alpha$ develops a power-law tail with an exponent $\alpha<2$ (see Fig. 3) typical of anomalous diffusion. The exponent α does not depend on σ; in all cases, we have found $\alpha\sim 1.1\pm 0.2$. This is a clear signature of an AT. We remark that, in agreement with the energy diffusion results of the previous section, the quantum decay is slower than the classical one. Quantum interference slows down the motion but it is not enough to fully localize the particle.

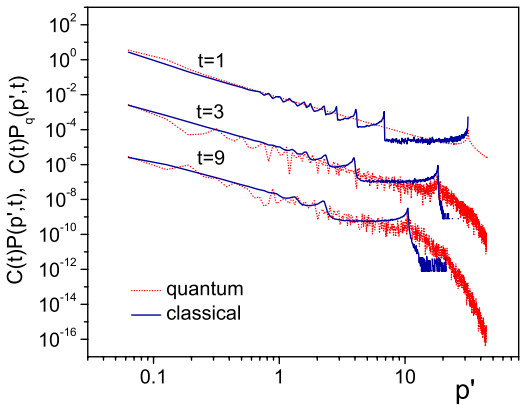

FIG. 4. (Color online) Comparison of the classical density of probability distribution $P(p',t)$ and its quantum counterpart $P_q(p',t)$ in the range $t<t_c\leqslant 10$, $p'=p/\sqrt{2Dt}$, $\sigma=10^{-3}$, and the bin width $\Delta p'=2/\sqrt{2D}\approx 0.063$. For the sake of clearness, the results for $t=3$ and $t=9$ are shifted by a factor $C(3)=10^{-3}$, and $C(9)=10^{-6}$, respectively; $C(1)=1$. As was expected, we observe agreement between classical and quantum results in the region $p'\leqslant 1$.

(iii) For $|p|>c(\sigma)\sqrt{2Dt}$ and $t>t_d$, $P_q(p,t)$ decays exponentially. This is an indication of full dynamical localization due to the differentiability of the potential.

From the above we can affirm that in order to observe typical features of an AT in the transport properties of our system, t_c and t_d must be well separated—namely, $t_d\gg t\gg t_c$. As is shown in Fig. 3 and Table I, this occurs provided that $\sigma\leqslant 0.05$. Thus for an experimental verification of the AT in cold atoms one has to manage to produce a bare step potential up to corrections of order $\sigma\leqslant 0.05$

C. Experimental verification

A natural question to ask is what is the minimum value of σ that it can be reached in experiments. Specifically, we wish to determine, for instance, the maximum number of terms in $V_1(q)$ that can be included experimentally. In principle [18] it is a challenging experimental task to built optical potentials with high slopes involving higher optical harmonics of the laser beam. The problem is that—for instance, for Cs—the fourth harmonic is already in the vacuum ultraviolet and difficult to produce. Moreover, higher-order harmonics are not resonant with the atom and need a much stronger intensity.

TABLE I. Time scales t_c and t_d for various values of σ.

σ	t_c	t_d
1×10^{-1}	7±4	11±3
5×10^{-2}	7±4	35±10
2×10^{-2}	7±4	50±25
1×10^{-2}	7±4	250±50
5×10^{-3}	8±4	410±100
2×10^{-3}	8±4	1300±250
1×10^{-3}	8±4	2000±400
5×10^{-4}	8±4	4800±1200

Thus it seems extremely hard to go beyond the first few harmonics. Another option is to use a kicked rotor with a smooth potential and three incommensurate frequencies. According to the results of [22], this model is mapped it onto a 3D Anderson model which is supposed to undergo an AT for a specific value of the coupling constant. However, in more than one dimension there is no clear evidence that this mapping is really accurate. For instance, the critical exponents at the AT are very different from the one found in the kicked rotor with three incommensurate frequencies [23].

A more promising alternative is to use a holographic mask to give a square-wave intensity profile [19]. This technique, combined with the recent introduction of spatial light modulators, permits the production of a very broad range of intensity patterns which act as an effective spatial potential for atoms. Moreover, the sharpness of the edges is limited only by diffraction effects of the order of the wavelength [18]. With the current techniques the potential of Eq. (3) could be produced in a window $\sigma\geqslant 10^{-2}$. On the other hand, quantum coherence in cold atoms is lost after a few thousand kicks. The experimental bounds are thus within the theoretical limits and, as a consequence, the AT can be studied by using ultracold atoms in optical lattices.

A final remark is in order. Signatures of an AT are not only found in the transport properties but also in the level statistics and the anomalous scaling of the eigenfunctions. In this paper we have focused only on the transport properties because our main motivation is to explore experimental signatures of the AT in ultracold atoms. Although not relevant for experiments, we would like to say a few words about the effect of a smoothed singularity on level statistics. We have recently [16] showed that in the limit $\sigma\to 0$ the level statistics associated to the spectrum of the Hamiltonian (3) is similar to that of a disordered conductor at the Anderson transition. For any finite σ deviations from this critical behavior are expected as a function of the parameter $\gamma=\sigma N$ where N is the size of the system. Spectral correlations of eigenvalues separated a distance $s\ll\gamma$ [with $s=(E_i-E_j)/\Delta$ and Δ the mean level spacing] are not affected by a finite σ. However, Poisson statistics due to the differentiability of the potential is expected for spectral correlations in the region $s\gg\gamma$.

In conclusion, we have explicitly shown that a kick rotator with a singular but slightly smoothed potential still has similar transport properties as those of a disordered conductor at the AT provided that the degree of smoothing is weak enough. The utilization of ultracold atoms in optical lattices offers the opportunity to investigate Anderson localization in general and the AT in particular in a setting free from many of the inconveniences that have plagued other experimental studies of the AT in the context of condensed matter physics.

ACKNOWLEDGMENTS

A.M.G. thanks D. A. Steck, J. F. Garreau, and T. Monteiro for illuminating explanations. A.M.G. acknowledges financial support from a Marie Curie Action, Contract No. MOIF-CT-2005-007300. J.W. acknowledges the support provided by the National University of Singapore.

[1] P. W. Anderson, Phys. Rev. **109**, 1492 (1958).
[2] E. Abrahams *et al.*, Phys. Rev. Lett. **42**, 673 (1979).
[3] K. B. Efetov, Adv. Phys. **32**, 53 (1983).
[4] M. Schreiber and H. Grussbach, Phys. Rev. Lett. **67**, 607 (1991); A. MacKinnon and B. Kramer, *ibid.* **47**, 1546 (1981); **81**, 268 (1998); Nucl. Phys. B **B525**, 738 (1998).
[5] H. Aoki, J. Phys. C **16**, L205 (1983); A. D. Mirlin *et al.*, Phys. Rev. E **54**, 3221 (1996); F. Evers and A. D. Mirlin, Phys. Rev. Lett. **84**, 3690 (2000); E. Cuevas *et al.*, *ibid.* **88**, 016401 (2001).
[6] B. I. Shklovskii, B. Shapiro, B. R. Sears, P. Lambrianides, and H. B. Shore, Phys. Rev. B **47**, 11487 (1993).
[7] V. E. Kravtsov and K. A. Muttalib, Phys. Rev. Lett. **79**, 1913 (1997); S. M. Nishigaki, Phys. Rev. E **59**, 2853 (1999).
[8] M. Janssen, Int. J. Mod. Phys. B **8**, 943 (1994); B. Huckestein, Rev. Mod. Phys. **67**, 357 (1995).
[9] B. Huckestein and R. Klesse, Phys. Rev. B **59**, 9714 (1999).
[10] F. L. Moore, J. C. Robinson, C. F. Bharucha, Bala Sundaram, and M. G. Raizen, Phys. Rev. Lett. **75**, 4598 (1995).
[11] F. M. Izrailev, Phys. Rep. **196**, 299 (1990).
[12] G. Casati, B. V. Chirikov, F. M. Izrailev, and J. Ford, in *Stochastic Behavior in Classical and Quantum Hamiltonian Systems*, edited by G. Casati and J. Ford, *Lecture Notes in Physics*, Vol. 93 (Springer, Berlin, 1979); B. V. Chirikov, F. M. Izrailev, and D. L. Shepelyansky, Sov. Sci. Rev. **2C**, 209 (1981).
[13] S. Fishman, D. R. Grempel, and R. E. Prange, Phys. Rev. Lett. **49**, 509 (1982).
[14] K. Drese and M. Holthaus, Phys. Rev. Lett. **78**, 2932 (1997).
[15] H. Ammann, R. Gray, I. Shvarchuck, and N. Christensen, Phys. Rev. Lett. **80**, 4111 (1998); B. G. Klappauf, W. H. Oskay, D. A. Steck, and M. G. Raizen, *ibid.* **81**, 4044 (1998); M. B. d'Arcy, R. M. Godun, M. K. Oberthaler, D. Cassettari, and G. S. Summy, *ibid.* **87**, 074102 (2001); J. Gong, H. J. Wrner, and P. Brumer, Phys. Rev. E **68**, 056202 (2003); H. Lignier, J. Chabe, D. Delande, J. C. Garreau, and P. Szriftgiser, Phys. Rev. Lett. **95**, 234101 (2005).P. H. Jones, M. M. A. Stocklin, G. Hur, , and T. S. Monteiro, Phys. Rev. Lett. **93**, 223002 (2004).
[16] A. M. Garcia-Garcia and J. Wang, Phys. Rev. Lett. **94**, 244102 (2005); Phys. Rev. E **73**, 036210 (2006); A. M. Garcia-Garcia, *ibid.* **72**, 066210 (2005); A. M. Garcia-Garcia and J. J. M. Verbaarschot, *ibid.* **67**, 046104 (2003).
[17] C. F. Bharucha, J. C. Robinson, F. L. Moore, Bala Sundaram, Qian Niu, and M. G. Raizen, Phys. Rev. E **60**, 3881 (1999).
[18] We thank J. F. Garreau and D. A. Steck (private communication).
[19] M. Mutzel *et al.*, Phys. Rev. Lett. **88**, 083601 (2002).
[20] A. J. Lichtenberg and M. A. Lieberman, *Regular and Chaotic Dynamics*, 2nd ed. (Springer-Verlag, New York, 1992).
[21] J. Klafter and G. Zumofen, Phys. Rev. E **49**, 4873 (1994).
[22] G. Casati, I. Guarneri, and D. L. Shepelyansky, Phys. Rev. Lett. **62**, 345 (1989).
[23] F. Borgonovi and D. L. Shepelyansky, Physica D **109**, 24 (1997).